Inorg. Chem. **2006**, *45*, 3057–3066

Developing the $\{M(CO)_3\}^+$ Core for Fluorescence Applications: Rhenium Tricarbonyl Core Complexes with Benzimidazole, Quinoline, and Tryptophan Derivatives

Lihui Wei,[†] John W. Babich,[‡] Wayne Ouellette,[†] and Jon Zubieta*,[†]

Department of Chemistry, Syracuse University, Syracuse, New York 13244, and Molecular Insight Pharmaceuticals Inc., 260 Second Street, Cambridge, Massachusetts 02142

Received October 6, 2005

Tridentate ligands derived from benzimidazole, quinoline, and tryptophan have been synthesized, and their reactions with $[NEt_4]_2[Re(CO)_3Br_3]$ have been investigated. The complexes **1**–**4** and **6** and **7** exhibit *fac*-$\{Re(CO)_3N_3\}$ coordination geometry in the cationic molecular units, while **5** exhibits *fac*-$\{Re(CO)_3N_2O\}$ coordination for the neutral molecular unit, where N_3 and N_2O refer to the ligand donor groups. The ligands bis(1-methyl-1*H*-benzoimidazol-2-ylmethyl)amine (**L1**), [bis(1-methyl-1*H*-benzoimidazol-2-ylmethyl)amino]acetic acid ethyl ester (**L2**), [bis(1-methyl-1*H*-benzoimidazol-2-ylmethy)amino]acetic acid methyl ester (**L3**), [bis(quinolin-2-ylmethyl)amino]acetic acid methyl ester (**L4**), 3-(1-methyl-1*H*-indol-3-yl)-2-[(pyridin-2-ylmethyl)amino]propionic acid (**L5**), 2-[bis(pyridin-2-ylmethyl)amino]-3-(1-methyl-1*H*-indol-3-yl)propionic acid (**L6**), and 2-[bis(quinolin-2-ylmethyl)amino]-3-(1-methyl-1*H*-indol-3-yl)propionic acid (**L7**) were obtained in good yields and characterized by elemental analysis, 1D and 2D NMR, and high-resolution mass spectrometry (HRMS). The rhenium complexes were obtained in 70–85% yields and characterized by elemental analysis, 1D and 2D NMR, HRMS, IR, UV, and luminescence spectroscopy, as well as X-ray crystallography for $[Re(CO)_3(\mathbf{L1})]Br$ (**1**), $\{[Re(CO)_3(\mathbf{L2})]Br\}_2 \cdot NEt_4Br \cdot 8.5H_2O$ ($\mathbf{3}_2 \cdot NEt_4Br \cdot 8.5H_2O$), $[Re(CO)_3(\mathbf{L4})]Br$ (**4**), and $[Re(CO)_3(\mathbf{L6})]Br$ (**6**). Crystal data for $C_{21}H_{19}BrN_5O_3Re$ (**1**): monoclinic, $P2_1/c$, $a = 13.1851(5)$ Å, $b = 16.1292(7)$ Å, $c = 10.2689(4)$ Å, $\beta = 99.353(1)°$, $V = 2154.8(2)$ Å^3, $Z = 4$. Crystal data for $C_{56}H_{73}Br_3N_{11}O_{18.50}Re_2$ ($\mathbf{3}_2 \cdot NEt_4Br \cdot 8.5H_2O$): monoclinic, $C2/c$, $a = 34.7760(19)$ Å, $b = 21.1711(12)$ Å, $c = 20.3376(11)$ Å, $\beta = 115.944(1)°$, $V = 13464.5(1)$ Å^3, $Z = 8$. Crystal data for $C_{26}H_{21}BrN_3O_5Re$ (**4**): monoclinic, $P2_1/c$, $a = 16.6504(6)$ Å, $b = 10.1564(4)$ Å, $c = 14.6954(5)$ Å, $\beta = 96.739(1)°$, $V = 2467.9(2)$ Å^3, $Z = 4$. Crystal data for $C_{27}H_{24}BrN_4O_5Re$ (**6**): monoclinic, $P2_1$, $a = 8.7791(9)$ Å, $b = 16.312(2)$ Å, $c = 8.9231(9)$ Å, $\beta = 90.030(1)°$, $V = 1277.8(2)$ Å^3, $Z = 2$.

Introduction

The continuing interest in the coordination chemistry of the group VII elements technetium and rhenium reflects the application of their radionuclides to the development of radiopharmaceuticals.[1] ^{99m}Tc has become the radioisotope of choice in diagnostic nuclear medicine because of its ideal nuclear properties ($E_{\gamma,\max} = 140$ keV; $t_{1/2} = 6$ h) and its ready availability from a commercial ^{99}Mo/^{99m}Tc generator.[2] The β-emitting radionuclides ^{186}Re ($E_{\max} = 1.07$ MeV; $t_{1/2} = 90$ h) and ^{188}Re ($E_{\max} = 2.12$ MeV; $t_{1/2} = 17$ h) of the group VII congener of technetium have become the logical choices for therapeutic applications.[3]

The chemistry of technetium and rhenium has been well documented.[1,2] Technetium and rhenium exhibit considerable chemical diversity, with complexes in oxidation states 1−

* To whom correspondence should be addressed. E-mail: jazubiet@syr.edu. Fax: +1 315 443 4070.
[†] Syracuse University.
[‡] Molecular Insight Pharmaceuticals Inc.

(1) (a) Arano, Y. *Ann. Nucl. Med.* **2002**, *16*, 79. (b) Johannsen, B. *Wiss.-Tech. Ber.—Forschungszent. Rossendorf* **2202**, *FZR-340*, 1. (c) Nicolini, M., Bandoli, G., Mazzi, U., Eds. *Technetium, Rhenium and Other Metals in Chemistry and Nuclear Medicine*; Raven Press: New York, 2000; p 5. (d) Nicolini, M., Bandoli, G., Mazzi, U., Eds. *Technetium and Rhenium in Chemistry and Nuclear Medicine;* Raven Press: New York, 1990. (e) Jurisson, S. S.; Lyden, J. D. *Chem. Rev.* **1999**, *99*, 2205. (f) Liu, S.; Edwards, O. S. *Chem. Rev.* **1999**, *99*, 2235. (g) Dilworth, J. R.; Parrott, S. J. *Chem. Soc. Rev.* **1998**, *27*, 43. (h) Hom, R. K.; Katzenellenbogen, J. A. *Nucl. Med. Biol*. **1997**, *24*, 485. (i) Eckelman, W. C. *Eur. J. Nucl. Med*. **1995**, *22*, 249. (j) Schwochan, K. *Angew. Chem., Int. Ed. Engl*. **1994**, *33*, 2258.
(2) (a) Kohlickova, M.; Jedinakova-Krizova, V.; Melichar, F. *Chem. Listy* **2000**, *94*, 151. (b) Blower, P. J.; Prakash, S. *Perspect. Bioinorg. Chem.* **1999**, *4*, 91. (c) Volkert, W. A.; Hoffman, T. J. *Chem. Rev*. **1999**, *99*, 2269. (d) Palmedo, H.; Guhlke, S.; Bender, H.; Sartor, J.; Schoeneich, G.; Risse, J.; Grunwalk, F.; Knapp, F. F., Jr.; Biersack, H. J. *Eur. J. Nucl. Med*. **2000**, *27*, 123.

10.1021/ic0517319 CCC: $33.50
Published on Web 03/02/2006

to 7+ having been reported.[2] This chemical versatility is reflected in a number of robust chemical cores that have been investigated for applications to radiopharmaceutical development.[2,4] The most extensively developed chemistry is that of the technetium and rhenium complexes of the metal−oxo $\{M^{V}O\}^{3+}$ core.[5] Most recently, the organometallic approach pioneered by Jaouen and co-workers[6] has resulted in the development of $\{M(CO)_3\}^{+}$ (M = Tc and Re) cores as platforms for target-specific radiopharmaceuticals.[7−9] Because the $\{M(CO)_3\}^{+}$ unit is readily available as the air-stable *fac*-$[M(CO)_3(H_2O)_3]^{+}$ species, a variety of functional groups, including amines, thioethers, imines, thiols and phosphines, will react with this reagent to displace the substitutionally labile aqua ligands.[10−12] The $\{M(CO)_3\}^{+}$ core is also attractive as a low-spin d^6 M(I) center, which is kinetically inert and possesses three facially disposed carbonyl donors that fix three coordination sites about the metal, leaving the three remaining facial positions available for substitution. The small size of the core allows labeling of low molecular weight biomolecules with high specific activities with retention of the biological activity and specificity.

We have recently reported on a series of bifunctional single amino acid chelates for labeling of the biomolecules with the $\{Tc(CO)_3\}^{+}$ and $\{Re(CO)_3\}^{+}$ cores.[11] Such amino acid analogues provide a tridentate donor set for chelation and an amino acid functionality for attachment to biomolecules and, consequently, can be readily incorporated into peptides using conventional solid-phase synthesis techniques.[13,14] Furthermore, we are investigating the bifunctional chelates that form fluorescent complexes with rhenium and also possess the ability to bind ^{99m}Tc.[15] Although the resolution of radioimaging techniques does not permit visualization at the cellular level, cellular targets can be identified by replacing the radioisotope with a fluorophore. This approach affords the opportunity to correlate the results of fluorescence microscopy with in vivo radioimaging studies because of the structural identity of the probes. Complementary radiopharmaceuticals and fluorescent probes based on the $\{M(CO)_3\}^{+}$ core, where M = Tc and Re, respectively, would then become readily available.

Highly conjugated compounds, such as quinoline, benzimidazole, and indole, can be used as fluorophores. In this work, we report the syntheses and characterization of rhenium tricarbonyl complexes with tridentate ligands derived from quinoline and benzimidazole. We also investigate a series of bifunctional chelators derived from indole-containing amino acid tryptophan and their complexes with the $\{Re(CO)_3\}^{+}$ core. The structures of $[Re(CO)_3(\mathbf{L1})]Br$ (**L1** = bis(1-methyl-1*H*-benzoimidazol-2-ylmethyl)amine), $[Re(CO)_3(\mathbf{L3})]Br$ (**L3** = [bis(1-methyl-1*H*-benzoimidazol-2-ylmethyl)amino]acetic acid methyl ester), $[Re(CO)_3(\mathbf{L4})]Br$ (**L4** = [bis(quinolin-2-ylmethyl)amino]acetic acid methyl ester), and $[Re(CO)_3(\mathbf{L6})]Br$ (**L6** = 2-[bis(pyridin-2-ylmethyl)amino]-3-(1-methyl-1*H*-indol-3-yl)propionic acid) are described. The luminescent properties of complexes **3**, **4**, **6**, and **7** are discussed.

Experimental Section

General Methods. All reagents and organic solvents used in this study are reagent-grade and were used without further purification. $[NEt_4]_2[ReBr_3(CO)_3]$[16] was prepared according to the literature method. ^{1}H and ^{13}C NMR spectra were recorded on a Bruker DPX 300 spectrometer; all peak positions are relative to tetramethylsilane. IR spectra were recorded as KBr pellets with a Perkin-Elmer series 1600 Fourier transform IR spectrometer in the region of 400−4000 cm^{-1} with polystyrene as the reference. HRMS spectra were obtained on a Kratos MS-890 mass spectrometer under electron

(3) (a) Weininger, J.; Ketring, A. R.; Deutsch, E.; Maxon, H. R.; Goeckler, W. R. *J. Nucl. Med.* **1983**, *24*, 125. (b) Wessels, B. W.; Rogus, R. D. *Med. Phys.* **1984**, *11*, 638. (c) Yorke, E. D.; Beaumier, P.; Wessels, B.; Fritzberg, A.; Morgan, A. *Nucl. Med. Biol.* **1991**, *18*, 827. (d) Vanderheyden, J. L.; Fritzberg, A. R.; Rao, T. N.; Kasina, S.; Srinivasan, A.; Rano, J. M.; Morgan, A. C. *J. Nucl. Med.* **1987**, *28*, 656.

(4) Banerjee, S. R.; Francesconi, L.; Valliant, J. F.; Babich, J. W.; Zubieta, J. *Nucl. Med. Biol.* **2005**, *32*, 1.

(5) (a) Johannsen, B.; Spies, H. *Top. Curr. Chem.* **1996**, *176*, 77. (b) Lister-James, J.; Moyen, B. R.; Dean, T. Q. *J. Nucl. Med.* **1996**, *40*, 233. (c) Meegalla, S. K.; Plossl, K.; Kung, M.-P.; Chumpradit, S.; Stevenson, A. D.; Kushner, S. A.; McElgin, W. T.; Mozley, D. P.; Kung, H. F. *J. Med. Chem.* **1997**, 9. (d) Hoepping, A.; Babich, J.; Zubieta, J.; Johnson, K. M.; Machile, S.; Kozikowski, A. P. *Bioorg. Med. Chem. Lett.* **1999**, *9*, 3211. (e) Zhuang, Z. P.; Plossl, K.; Kung, M.-P.; Mu, M.; Kung, H. F. *Nucl. Med. Biol.* **1999**, *26*, 217. (f) Rajagopalan, R.; Grumman, G. D.; Bugaj, J.; Hallemann, L. S.; Webb, E. G.; Marmion, M. E.; Venderheyden, J. L.; Srinivasan, A. *Bioconjugate Chem.* **1997**, *8*, 407.

(6) (a) Fish, R. H.; Jaouen, G. *Organometallics* **2003**, *22*, 2166. (b) Schibli, R.; Schubiger, P. A. *Eur. J. Nucl. Med.* **2002**, *29*, 1529. (c) Le Bidean, F.; Perez-Luna, A.; Marrot, J.; Rager, M.-N.; Stephan, E.; Top, S.; Jaouen, G. *Tetrahedron* **2001**, *57*, 3939. (d) Salman, M.; Gunn, M.; Gorbi, A.; Top, S.; Jaouen, G. *Bioconjugate Chem.* **1993**, *4*, 425. (e) Top, S.; Hafa, E. H.; Vessières, A.; Quincy, J.; Vaisserman, J.; Hughes, D. W.; McGlinchey, M. J.; Mornon, J.-P.; Thoreau, E.; Jaouen, G. *J. Am. Chem. Soc.* **1995**, *117*, 8372.

(7) (a) Alberto, R.; Schibili, R.; Egli, A.; Schubiger, A. P.; Abram, U.; Kaden, T. A. *J. Am. Chem. Soc.* **1998**, *120*, 7987. (b) Alberto, R.; Schibli, R.; Angst, D.; Schubiger, P. A.; Abram, U.; Abram, S.; Kaden, T. L. A. *Trans. Mater. Chem.* **1997**, *22*, 597. (c) Alberto, R.; Schibli, R.; Schubiger, A. P. *J. Am. Chem. Soc.* **1999**, *212*, 6076. (d) Waibei, R.; Alberto, R.; Willude, J.; Finnern, R.; Schibli, R.; Stichelberger, A.; Egli, A.; Abram, U.; Mach, J. P.; Pluckthern, A.; Schubiger, P. A. *Nat. Biotechnol.* **1999**, *17*, 897. (e) Amann, A.; Decristoforo, C.; Ott, I.; Wenger, M.; Bader, D.; Alberto, R.; Putz, G. *Nucl. Med. Biol.* **2001**, *28*, 243. (f) Schibli, R.; LaBelle, R.; Alberto, R.; Garcia-Garayoa, L.; Ortner, K.; Abram, U.; Schubiger, P. A. *Bioconjugate Chem.* **2000**, *11*, 345. (g) Wald, J.; Alberto, R.; Ortner, K.; Andreia, L. *Angew. Chem., Int. Ed.* **2001**, *40*, 3062.

(8) LeBidean, F.; Salmain, M.; Top, S.; Jaouen, G. *Chem.—Eur. J.* **2001**, *7*, 2289.

(9) Synadau, T. W.; Edwards, W. B.; Anderson, C. J.; Welch, M. J.; Kaltzenellenbogen, J. A. *Nucl. Med. Biol.* **1998**, *26*, 1.

(10) Kramer, D. J.; Davison, A.; Davis, W. M.; Jones, A. G. *Inorg. Chem.* **2002**, *41*, 6181.

(11) Banerjee, S. R.; Levadala, M. K.; Lazarova, N.; Wei, L.; Valliant, J. F.; Stephenson, K. A.; Babich, J. W.; Maresca, K. P.; Zubieta, J. *Inorg. Chem.* **2002**, *41*, 6417.

(12) Alberto, R.; Schibili, R.; Waihel, R.; Schubiger, P. A. *Coord. Chem. Rev.* **1999**, *190−192*, 901.

(13) Stephenson, K. A.; Valliant, J. F.; Zubieta, J.; Banerjee, S. R.; Levadala, M. K.; Taggart, L.; Ryan, L.; MaFarlane, N.; Boreham, D. R.; Babich, J. W.; Maresca, K. P. *J. Nucl. Med.* **2003**, *44*, 48p.

(14) Stephenson, K. A.; Zubieta, J.; Banerjee, S. R.; Levadala, M. K.; Taggart, L.; Ryan, L.; McFarlane, N.; Boreham, D. R.; Maresca, K. P.; Babich, J. W.; Valliant, J. F. *Bioconjugate Chem.* **2004**, *15*, 128.

(15) Stephenson, K. A.; Banerjee, S. R.; Besanger, T.; Sogbein, O. O.; Levadala, M. K.; McFarlane, N.; Lemon, J. A.; Boreham, D. R.; Maresca, K. P.; Brennan, J. D.; Babich, J. W.; Zubieta, J.; Valliant, J. F. *J. Am. Chem. Soc.* **2004**, *126*, 8598.

(16) Alberto, R.; Egli, A.; Abram, U.; Hegetschweiler, K.; Gramlich, V.; Schubiger, P. A. *J. Chem. Soc., Dalton Trans.* **1994**, 2815.

Scheme 1

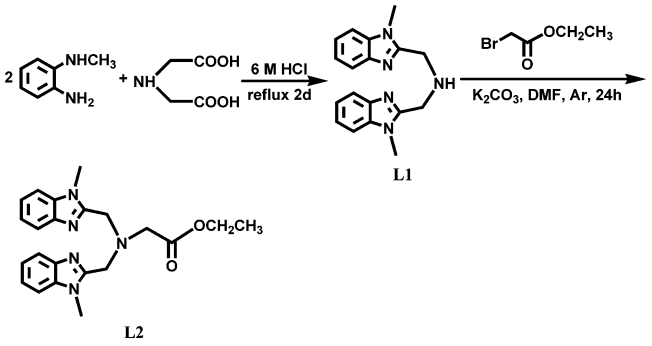

impact ionization conditions. Carbon, hydrogen, and nitrogen analyses were carried out by Oneida Research Services, Whitesboro, NY. Electronic absorption spectra were recorded on a Varian Cary 50 Bio UV−visible spectrophotometer. Measurements were performed with baseline correction using matched quartz cuvettes. Steady-state excitation and emission spectra and lifetime measurements were obtained on a Photon Technology International spectrofluorometer. XenoFlash pulsed light was the excitation source for emission lifetime measurements. Luminescence quantum yields were measured by the optical dilute method[17] using an aerated aqueous solution of $[Ru(bpy)_3]Cl_2$ ($\Phi = 0.028$)[18] as the standard solution.

Ligand Syntheses. Bis(1-methyl-1*H*-benzoimidazol-2-ylmethyl)amine (L1). Ligand **L1** was prepared by Phillips condensation according to the literature procedure[19] with minor modifications (Scheme 1).

[Bis(1-methyl-1*H*-benzoimidazol-2-ylmethyl)amino]acetic Acid Ethyl Ester (L2). L1 (0.469 g, 1.88 mmol) was dissolved in anhydrous dimethylformamide (DMF; 10 mL). Potassium carbonate (0.521 g, 3.77 mmol) and ethyl bromoacetate (0.377 g, 2.26 mmol) were added to the solution under an argon atmosphere. The suspension was protected from light and allowed to stir at 30 °C, under argon, for 24 h. Water was added, and the mixture was extracted with chloroform. The organic layer was evaporated to dryness. The residue was dissolved in dichloromethane and carefully layered with hexane. Crystalline pure product was obtained after 1 week. Yield: 0.24 g (0.72 mmol, 40%). ^{1}H NMR (δ (ppm), $CDCl_3$): 7.65−7.64 (m, 2H, bzim (benzimidazole)), 7.20−7.12 (m, 6H, bzim), 4.02−3.95 (s+q, 6H, bzimCH_2, CO_2CH_2), 3.59 (s, 6H, NCH_3), 3.44 (s, 2H, NCH_2), 1.13 (t, 3H, CH_2CH_3). ^{13}C NMR (δ (ppm), $CDCl_3$): 170.89 (CO_2), 150.86, 142.33, 136.33, 123.03, 122.27, 119.88, 109.44, 60.88, 55.15, 51.27, 29.91, 14.28.

[Bis(1-methyl-1*H*-benzoimidazol-2-ylmethyl)amino]acetic Acid Methyl Ester (L3). Aminoacetic acid methyl ester hydrochloride (0.189 g, 1.51 mmol) and 1-(methylformyl)benzimidazole (0.483 g, 3.01 mmol) were mixed in 1,2-dichloroethane (DCE). Sodium triacetoxyborohydride (0.958 g, 4.52 mmol) was then added. The suspension was stirred at room temperature under argon for 4 h. The reaction mixture was quenched by adding a saturated sodium bicarbonate solution and extracted with dichloromethane. After concentration of the dichloromethane layer under vacuum, the crude product was purified by silica gel column chromatography using CH_3OH/CH_2Cl_2 (3/96) to give **L3**. Yield: 0.342 g (0.906 mmol, 60%). ^{1}H NMR (δ (ppm), $CDCl_3$): 7.71−7.68 (m, 2H, bzim), 7.23−7.19 (m, 6H, bzim), 4.01 (s, 4H, bzimCH_2), 3.70 (s, 3H, CO_2CH_3), 3.57 (s, 6H, NCH_3), 3.47 (s, 2H, NCH_2). ^{13}C NMR (δ (ppm), $CDCl_3$): 172.63 (CO_2), 152.16, 143.53, 137.59, 124.43, 123.68, 121.12, 110.84, 58.34, 56.15, 52.42, 31.19. HRMS. Calcd for $C_{21}H_{23}N_5O_2Na^+$ (M + Na^+): 400.174 393. Found: 400.174 15.

[Bis(quinolin-2-ylmethyl)amino]acetic Acid Methyl Ester (L4). The ligand was prepared by a procedure similar to that described in the case of **L3**, except that 2-quinolinecarboxaldehyde was used instead of 1-(methylformyl)benzimidazole. Yield: 86%. ^{1}H NMR (δ (ppm), $CDCl_3$): 8.05 (t, $J = 8.1$ Hz, 4H, Qu), 7.72 (t, $J = 8.7$ Hz, 4H, Qu), 7.61 (t, $J = 6.9$ Hz, 2H, Qu), 7.42 (t, $J = 6.9$ Hz, 2H, Qu), 4.16 (s, 4H, QuCH_2), 3.63 (s, 3H, CO_2CH_3), 3.52 (s, 2H, NCH_2). ^{13}C NMR (δ (ppm), $CDCl_3$): 171.64 (CO_2), 159.71, 147.40, 136.58, 129.42, 128.87, 127.51, 127.38, 126.23, 121.26, 60.76, 55.01, 51.49. HRMS. Calcd for $C_{23}H_{21}N_3O_2Na^+$ (M + Na^+): 394.152 595. Found: 394.154 61.

3-(1-Methyl-1*H*-indol-3-yl)-2-[(pyridin-2-ylmethyl)amino]propionic Acid (L5). L5 was prepared by a procedure similar to that described in the case of **L3**, except that 2-pyridinecarboxaldehyde and 1-methyl-L-tryptophan were used instead of 1-(methylformyl)-benzimidazole and aminoacetic acid methyl ester. After the reaction mixture was quenched with a saturated sodium bicarbonate solution and extracted with dichloromethane, a white precipitate appeared in both the inorganic and organic layers. The precipitate was filtered and dried to give a pure product. Yield: 38%. ^{1}H NMR (δ (ppm), CD_3OD): 8.20 (d, $J = 5.1$ Hz, 1H, Py), 7.71 (t, $J = 7.5$ Hz, 1H, Py), 7.61 (d, $J = 7.8$ Hz, 1H, In (indole)), 7.37 (d, $J = 8.1$ Hz, 1H, In), 7.25−7.17 (m, 3H, Py + In), 7.16 (s, 1H, In), 7.03 (t, $J = 7.8$ Hz, 1H, In), 4.30 (d, $J = 15$ Hz, 1H, PyCH_2), 4.18 (d, $J = 15$ Hz, 1H, PyCH_2), 3.89 (q, $J = 9$ Hz, 1H, $CHCO_2$), 3.79 (s, 3H, NCH_3), 3.55 (dd, 1H, InCH_2), 3.27 (dd, 1H, InCH_2). ^{13}C NMR (δ (ppm), CD_3OD): 174.81, 153.85, 150.16, 139.02, 138.70, 129.76, 129.25, 124.62, 124.10, 122.98, 120.28, 119.94, 110.50, 109.31, 64.08, 51.57, 32.96, 28.44. HRMS. Calcd for $C_{18}H_{19}N_3O_2Na^+$ (M + Na^+): 332.136 945. Found: 332.137 764.

2-[Bis(pyridin-2-ylmethyl)amino]-3-(1-methyl-1*H*-indol-3-yl)-propionic Acid (L6). 2-(Chloromethyl)pyridine hydrochloride (2.67 g, 16.3 mmol) and 1-methyl-L-tryptophan (1.69 g, 7.77 mmol) were dissolved in water and stirred at room temperature for 5 days, with the addition of a 5 M aqueous NaOH solution at intervals to maintain the pH at 8−10. The resulting solution was extracted with ethyl acetate. The water layer was acidified to pH 6 with HCl, extracted with chloroform, and concentrated under vacuum. The residue was purified by silica gel column chromatography using CH_3OH/CH_2Cl_2 (1/99) to give **L6**. Yield: 1.91 g (4.77 mmol, 62%). ^{1}H NMR (δ (ppm), $CDCl_3$): 8.46 (d, $J = 4.5$ Hz, 2H, Py), 7.49 (t, $J = 7.2$ Hz, 2H, Py), 7.42 (d, $J = 8.1$ Hz, 1H, In), 7.28 (d, $J = 7.2$ Hz, 1H, In), 7.21−7.17 (m, 3H, Py + In), 7.11 (t, $J = 6$ Hz, 2H, Py), 7.01 (t, $J = 7.5$ Hz, 1H, In), 6.94 (s, 1H, In), 4.12 (dd, 4H, PyCH_2), 3.93 (t, $J = 7.5$ Hz, 1H, $CHCO_2$), 3.53−3.47 (m, 1H, InCH_2), 3.27−3.19 (m, 1H, InCH_2). ^{13}C NMR (δ (ppm), $CDCl_3$): 175.27, 159.46, 148.18, 137.36, 137.13, 128.35, 128.05, 123.16, 122.50, 122.03, 121.61, 118.91, 111.24, 109.42, 65.15, 56.48, 32.84, 25.11. HRMS. Calcd for $C_{24}H_{24}N_4O_2Na^+$ (M + Na^+): 423.179 144. Found: 423.182 958.

2-[Bis(quinolin-2-ylmethyl)amino]-3-(1-methyl-1*H*-indol-3-yl-)propionic Acid (L7). L7 was prepared by a procedure similar to that described in the case of **L3**, except that 2-quinolinecarboxaldehyde and 1-methyl-L-tryptophan were used instead of 1-(methylformyl)benzimidazole and aminoacetic acid methyl ester. Yield: 55%. ^{1}H NMR (δ (ppm), $CDCl_3$): 8.05 (d, $J = 8.7$ Hz, 2H, Qu), 7.84 (d, $J = 8.7$ Hz, 2H, Qu), 7.64−7.60 (m, 3H, Qu + In), 7.42 (t, $J = 7.8$ Hz, 4H, Qu), 7.22−7.19 (m, 3H, Qu + In), 7.12 (t, $J =$

(17) Demas, J. N.; Crosby, G. A. *J. Phys. Chem.* **1971**, *75*, 991.
(18) Nakamaru, K. *Bull. Chem. Soc. Jpn.* **1982**, *55*, 2697.
(19) (a) Casella, L.; Carugo, O. *Inorg. Chem.* **1996**, *35*, 1101. (b) Sivagnanam, U.; Pandiyan, T.; Palaniadavar, M. *Ind. J. Chem.* **1993**, *32B*, 572.

7.2 Hz, 1H, In), 6.99 (s, 1H, In), 6.92 (t, J = 7.2 Hz, 1H, In), 4.28 (dd, 4H, $QuCH_2$), 4.10 (t, J = 8.1 Hz, 1H, $CHCO_2$), 3.63 (s, 3H, NCH_3), 3.60−3.53 (m, 1H, $InCH_2$), 3.54−3.28 (m, 1H, $InCH_2$). ^{13}C NMR (δ (ppm), $CDCl_3$): 175.76, 160.00, 146.71, 137.34, 137.08, 130.07, 128.56, 128.02, 127.84, 127.70, 127.43, 126.66, 121.60, 120.63, 118.95, 118.61, 110.96, 109.43, 66.11, 56.92, 32.77, 24.07. HRMS. Calcd for $C_{32}H_{28}N_4O_2Na^+$ (M^+): 523.210 444. Found: 523.213 54.

Syntheses of Rhenium Complexes of the Ligands L1−L7. The complexes were prepared by similar procedures. A representative synthesis for complex **1**) is presented in detail.

[Re(CO)$_3$(L1)]Br (1). To a stirred solution of $[NEt_4]_2[Re(CO)_3Br_3]$ (0.105 g, 0.137 mmol) in 20 mL of methanol was added **L1** (0.0340 g, 0.137 mmol) in 2 mL of methanol. The solution was refluxed for 3 h. White solid forms after cooling of the reaction mixture to room temperature. The white solid was filtered and dissolved in a minimum amount of hot methanol. After the methanol solution was cooled in a refrigerator, light-yellow fine crystals suitable for X-ray crystallography were obtained. Yield: 0.038 g (0.109 mmol, 80%). Anal. Calcd (found) for $C_{21}H_{19}BrN_5O_3Re$: C, 38.48 (38.27); H, 2.92 (3.06); N, 10.68 (10.49). ^{1}H NMR (δ (ppm), CD_3OD): 7.91−7.88 (m, 2H, bzim), 7.54−7.51 (m, 2H, bzim), 7.41−7.35 (m, 4H, bzim), 5.11−4.89 (dd, 4H, bzimCH_2), 3.83 (s, 6H, NCH_3). ^{13}C NMR (δ (ppm), CD_3OD): 197.76, 196.35 (*fac*-Re(CO)$_3$), 158.27, 144.71, 140.40, 128.14, 125.50, 121.50, 112.00, 46.05, 30.48. IR (KBr, ν/cm^{-1}): 2024, 1878 (ν(*fac*-Re(CO)$_3$)). HRMS. Calcd for $C_{21}H_{19}N_5O_3Re^+$ (M^+): 576.101 192. Found: 576.102 21.

[Re(CO)$_3$(L2)]Br (2). Yield: 82%. The color of the complex is light yellow. Anal. Calcd (found) for $C_{25}H_{25}BrN_5O_5Re$: C, 40.49 (40.62); H, 3.40 (3.55); N, 9.44 (9.21). ^{1}H NMR (δ (ppm), CD_3OD): 7.93−7.91 (m, 2H, bzim), 7.65−7.62 (m, 2H, bzim), 7.51−7.42 (m, 4H, bzim), 5.64 (d, J = 17.4 Hz, 2H, bzimCH_2), 5.28 (d, J = 17.4 Hz, bzimCH_2), 4.97 (s, 2H, NCH_2), 4.23 (q, J = 14.4 Hz, 2H, CO_2CH_2), 3.99 (s, 6H, NCH_3), 1.41 (t, J = 13.8 Hz, 3H, CH_3). ^{13}C NMR (δ (ppm), CD_3OD): 197.49, 196.25 (*fac*-Re(CO)$_3$), 169.98 (CO_2), 159.41, 141.15, 136.38, 125.87, 125.72, 118.24, 112.57, 68.96, 63.30, 61.98, 32.71, 14.55. IR (KBr, ν/cm^{-1}): 2023, 1899 (ν(*fac*-Re(CO)$_3$)).

[Re(CO)$_3$(L3)]Br (3). Yield: 79%. Light yellow crystals were obtained by dissolution of the compound in dichloromethane and careful layering of the solution with pentane. Anal. Calcd (found) for $C_{24}H_{23}BrN_5O_5Re$: C, 39.63 (39.87); H, 3.19 (3.35); N, 9.63 (9.47). ^{1}H NMR (δ (ppm), $CDCl_3$): 7.70−7.67 (m, 2H, bzim), 7.32−7.19 (m, 6H, bzim), 5.05−4.86 (dd, 4H, bzimCH_2), 4.74 (s, 2H, NCH_2), 3.90 (s, 6H, NCH_3), 3.71 (s, 3H, CO_2CH_3). ^{13}C NMR (δ (ppm), $CDCl_3$): 195.64, 194.76 (*fac*-Re(CO)$_3$), 168.31 (CO_2), 157.18, 139.84, 134.72, 124.65, 117.41, 111.04, 67.29, 61.05, 53.03, 32.72. IR (KBr, ν/cm^{-1}): 2024, 1910 (ν(*fac*-Re(CO)$_3$)). HRMS. Calcd for $C_{24}H_{23}N_5O_5Re^+$ (M^+): 648.125 115. Found: 648.124 07. Recrystallization of **3** gave X-ray-quality crystals of formulation $\mathbf{3}_2{\cdot}NEt_4Br{\cdot}8.5H_2O$.

[Re(CO)$_3$(L4)]Br (4). Yield: 76%. The compound was dissolved in dichloromethane, and the solution was carefully layered with hexane. Yellow fine crystals suitable for X-ray crystallography analysis were obtained. Anal. Calcd (found) for $C_{26}H_{21}BrN_3O_5Re$: C, 43.28 (43.41); H, 2.93 (3.11); N, 5.82 (5.67). ^{1}H NMR (δ (ppm), $CDCl_3$): 8.28 (t, J = 8.7 Hz, 4H, Qu), 7.82−7.59 (m, 6H, Qu), 7.49 (t, J = 7.5 Hz, 2H, Qu), 5.59 (d, J = 18 Hz, 2H, $QuCH_2$), 5.23 (d, J = 18 Hz, 2H, $QuCH_2$), 4.82 (s, 2H, NCH_2), 3.54 (s, 3H, CO_2CH_3). ^{13}C NMR (δ (ppm), $CDCl_3$): 195.07, 193.45 (*fac*-Re(CO)$_3$), 168.25 (CO_2), 164.41, 146.47, 141.39, 132.81, 129.56, 128.05, 127.94, 119.41, 70.50, 66.01, 52.61. IR (KBr, ν/cm^{-1}): 2032, 1896 (ν(*fac*-Re(CO)$_3$)). HRMS. Calcd for $C_{26}H_{21}N_3O_5Re^+$ (M^+): 642.103 317. Found: 642.101 32.

[Re(CO)$_3$(L5)] (5). Yield: 83%. The color of the complex is light yellow. Anal. Calcd (found) for $C_{21}H_{18}N_3O_5Re$: C, 43.59 (43.61); H, 3.14 (3.31); N, 7.26 (7.12). ^{1}H NMR (δ (ppm), $CDCl_3$): 8.79 (d, J = 4.8 Hz, 1H, Py), 7.84 (t, J = 7.8 Hz, 1H, Py), 7.69 (d, J = 7.8 Hz, 1H, Py), 7.42−7.11 (m, 6H, Py + In, In), 4.56−4.53 (m, 1H, $PyCH_2$), 4.32−4.27 (m, 1H, $PyCH_2$), 4.06−4.02 (m, $CHCO_2$), 3.85 (s, 3H, NCH_3), 3.62−3.53 (m, 1H, $InCH_2$), 3.10−3.05 (m, 1H, $InCH_2$). ^{13}C NMR (δ (ppm), $CDCl_3$): 197.01, 196.65, 196.38 (*fac*-Re(CO)$_3$), 181.78 (CO_2), 158.02, 152.94, 139.92, 137.95, 129.74, 126.99, 125.71, 123.01, 122.81, 120.09, 118.72, 110.12, 107.03, 65.56, 63.51, 33.15, 29.42. IR (KBr, ν/cm^{-1}): 2024, 1923, 1880 (ν(*fac*-Re(CO)$_3$)). HRMS. Calcd for $C_{21}H_{18}N_3O_5ReNa^+$ (M + Na^+): 602.069 609. Found: 602.073 89.

[Re(CO)$_3$(L6)]Br (6). Yield: 75%. Light-yellow crystals suitable for X-ray crystallography were obtained by slow diffusion of hexane into a concentrated solution of complex **6**. Anal. Calcd (found) for $C_{27}H_{24}BrN_4O_5Re$: C, 43.20 (43.39); H, 3.22 (3.38); N, 7.46 (7.29). ^{1}H NMR (δ (ppm), $CDCl_3$): 8.58 (m, 2H, Py), 7.74−7.60 (m, 5H, Py + In), 7.27−7.10 (m, 4H, Py + In), 7.03 (t, J = 7.6 Hz, 1H, In), 6.93 (t, J = 7.8 Hz, 1H, In), 5.65−5.28 (m, 2H, $PyCH_2$), 4.78−4.40 (m, 2H, $PyCH_2$), 3.76−3.71 (m, 1H, $CHCO_2$), 3.58 (s, 3H, NCH_3), 3.51−3.46 (m, 1H, $InCH_2$), 3.24−3.20 (m, 1H, $InCH_2$). ^{13}C NMR (δ (ppm), $CDCl_3$): 195.53, 194.77, 194.60 (*fac*-Re(CO)$_3$), 171.46 (CO_2), 160.56, 151.00, 140.35, 136.69, 128.82, 127.33, 125.72, 124.53, 121.59, 119.11, 118.69, 109.33, 107.04, 52.65, 49.59, 32.79, 26.46. IR (KBr, ν/cm^{-1}): 2026, 1932 (ν(*fac*-Re(CO)$_3$)). HRMS. Calcd for $C_{27}H_{24}N_4O_5Re^+$ (M^+): 671.129 866. Found: 671.129 07.

[Re(CO)$_3$(L7)]Br (7). Yield: 70%. The color of the complex is yellow. Anal. Calcd (found) for $C_{35}H_{28}BrN_4O_5Re$: C, 49.41 (49.53); H, 3.32 (3.51); N, 6.59 (6.43). ^{1}H NMR (δ (ppm), $CDCl_3$): 8.77 (d, J = 9 Hz, 2H, Qu), 8.38 (d, J = 8.8 Hz, 2H, Qu), 8.20−7.62 (m, 7H, Qu + In), 7.22−6.93 (m, 5H, Qu + In), 6.71 (d, J = 8.1 Hz, 1H, In), 5.46−5.04 (m, 4H, $QuCH_2$), 4.56 (t, 1H, $CHCO_2$), 3.32−3.22 (m, 1H, $InCH_2$), 2.94 (s, 3H, NCH_3), 2.22−2.17 (m, 1H, $InCH_2$). ^{13}C NMR (δ (ppm), $CDCl_3$): 194.58, 193.98, 193.21 (*fac*-Re(CO)$_3$), 181.46 (CO_2), 162.70, 154.83, 139.00, 138.12, 132.42, 130.90, 129.66, 128.43, 128.03, 127.71, 123.16, 121.91, 119.19, 118.71, 117.61, 109.40, 109.06, 69.27, 54.97, 32.05, 23.17. IR (KBr, ν/cm^{-1}): 2020, 1905 (ν(*fac*-Re(CO)$_3$)). HRMS. Calcd for $C_{35}H_{28}N_4O_5Re^+$ (M^+): 771.161 166. Found: 771.160 68.

X-ray Crystal Structure Determinations of Complexes 1, $\mathbf{3}_2{\cdot}NEt_4Br{\cdot}8.5H_2O$, 4, and 6. The selected crystals of the complexes were studied on a Bruker diffractometer equipped with the SMART CCD system,[20] using graphite-monochromated Mo Kα radiation (λ = 0.710 73 Å). The data collections were carried out at 90(5) K. The data were corrected for Lorentz and polarization effects, and absorption corrections were made using *SADABS*.[21] All calculations were performed using *SHELXTL96*.[22] The structures were solved by direct methods, and all of the non-hydrogen atoms were located from the initial solution. After all of the non-hydrogen atoms in the structure were located, the model was refined against F^2, initially using isotropic and later anisotropic thermal displacement parameters until the final value of Δ/σ_{max} was less than 0.001. At this point, the hydrogen atoms were located from the electron

(20) *Smart Software Reference Manual*; Siemens Analytical X-ray Instruments, Inc.: Madison, WI, 1994.
(21) Sheldrick, G. M. *SADABS: Program for Empirical Absorption Correction*; University of Göttingen: Göttingen, Germany, 1996.
(22) Sheldrick, G. M. *SHELXL96: Program for Refinement of Crystal Structures*; University of Göttingen: Göttingen, Germany, 1996.

Table 1. Summary of Crystal Data for Complexes **1**, $\mathbf{3}_2 \cdot NEt_4Br \cdot 8.5H_2O$, **4**, and **6**

	1	$\mathbf{3}_2 \cdot NEt_4Br \cdot 8.5H_2O$	**4**	**6**
formula	$C_{21}H_{19}BrN_5O_3Re$	$C_{56}H_{73}Br_3N_{11}O_{18.5}Re_2$	$C_{26}H_{21}BrN_3O_5Re$	$C_{27}H_{24}BrN_4O_5Re$
fw	655.52	1808.40	721.57	750.61
space group	$P2_1/c$	$C2/c$	$P2_1/c$	$P2_1$
T (K)	90	90	90	90
a (Å)	13.1851(5)	34.7760(19)	16.6504(6)	8.7791(9)
b (Å)	16.1292(7)	21.1711(12)	10.1564(4)	16.312(2)
c (Å)	10.2689(4)	20.3376(11)	14.6954(5)	8.9231(9)
β (deg)	99.353(1)	115.944(1)	96.739(1)	90.030(1)
V (Å^3)	2154.8(2)	13464.5(1)	2467.9(2)	1277.8(2)
Z	4	8	4	2
D_{calc} (g cm^{-3})	2.021	1.784	1.942	1.951
μ (mm^{-1})	7.527	5.390	6.586	6.365
R1[a]	0.0247	0.0612	0.0374	0.0407
wR2[a]	0.0463	0.1516	0.0559	0.0814

[a] $R1 = \sum||F_o| - |F_c||/\sum|F_o|$; $wR2 = [\sum w(F_o^2 - F_c^2)^2/\sum w(F_o^2)^2]^{1/2}$.

Table 2. Selected Bond Lengths [Å] and Angles [deg] for Complexes **1**, $\mathbf{3}_2 \cdot NEt_4Br \cdot 8.5H_2O$, **4**, and **6**

1		$\mathbf{3}_2 \cdot NEt_4Br \cdot 8.5H_2O$		**4**		**6**	
Re1−C2	1.909(2)	Re1−C3	1.890(13)	Re1−C1	1.903(3)	Re1−C2	1.871(10)
Re1−C1	1.917(2)	Re1−C2	1.899(10)	Re1−C2	1.918(3)	Re1−C3	1.898(10)
Re1−C3	1.927(2)	Re1−C1	1.929(14)	Re1−C3	1.919(3)	Re1−C1	1.905(10)
Re1−N2	2.1498(15)	Re1−N1	2.144(10)	Re1−N2	2.217(2)	Re1−N2	2.158(6)
Re1−N4	2.1508(16)	Re1−N4	2.157(8)	Re1−N3	2.231(2)	Re1−N1	2.178(7)
Re1−N1	2.2274(16)	Re1−N3	2.266(9)	Re1−N1	2.237(2)	Re1−N3	2.282(6)
C2−Re1−C1	89.26(8)	C3−Re1−C2	85.0(4)	C1−Re1−C2	82.67(11)	C2−Re1−C3	86.4(4)
C2−Re1−C3	90.00(8)	C3−Re1−C1	89.8(6)	C1−Re1−C3	85.72(11)	C2−Re1−C1	88.0(4)
C1−Re1−C3	89.63(8)	C2−Re1−C1	89.6(5)	C2−Re1−C3	88.92(10)	C3−Re1−C1	87.6(4)
C2−Re1−N2	98.58(7)	C3−Re1−N1	100.2(5)	C1−Re1−N2	103.21(9)	C2−Re1−N2	96.3(3)
C1−Re1−N2	94.50(7)	C2−Re1−N1	92.5(4)	C2−Re1−N2	172.88(9)	C3−Re1−N2	89.7(3)
C3−Re1−N2	170.50(7)	C1−Re1−N1	169.9(4)	C3−Re1−N2	95.48(9)	C1−Re1−N2	174.8(4)
C2−Re1−N4	98.88(7)	C3−Re1−N4	100.2(4)	C1−Re1−N3	103.44(9)	C2−Re1−N1	94.7(3)
C1−Re1−N4	171.04(7)	C2−Re1−N4	174.5(4)	C2−Re1−N3	97.12(9)	C3−Re1−N1	175.5(3)
C3−Re1−N4	94.09(7)	C1−Re1−N4	92.1(4)	C3−Re1−N3	169.56(9)	C1−Re1−N1	96.7(3)
N2−Re1−N4	80.65(6)	N1−Re1−N4	85.0(3)	N2−Re1−N3	77.72(7)	N2−Re1−N1	85.9(2)
C2−Re1−N1	172.90(7)	C3−Re1−N3	172.9(4)	C1−Re1−N1	178.46(9)	C2−Re1−N3	167.8(4)
C1−Re1−N1	94.72(7)	C2−Re1−N3	101.6(4)	C2−Re1−N1	96.32(9)	C3−Re1−N3	104.1(3)
C3−Re1−N1	95.89(7)	C1−Re1−N3	92.9(4)	C3−Re1−N1	93.11(9)	C1−Re1−N3	99.1(4)
N2−Re1−N1	75.27(6)	N1−Re1−N3	77.0(3)	N2−Re1−N1	77.88(7)	N1−Re1−N3	74.3(3)
N4−Re1−N1	76.80(6)	N4−Re1−N3	73.1(3)	N3−Re1−N1	77.81(8)		

Scheme 2

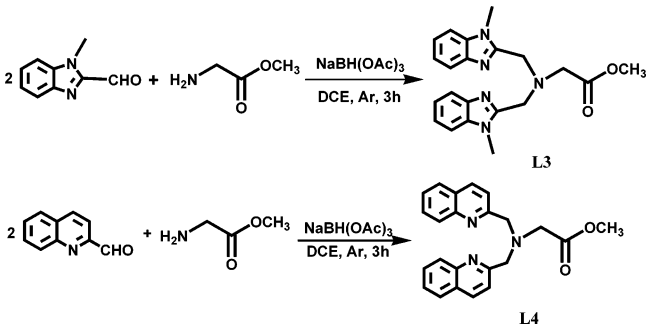

Scheme 3

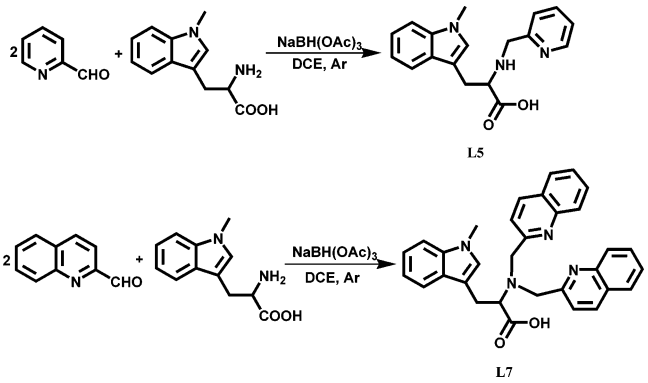

density difference map, and a final cycle of refinements was performed, until the final value of Δ/σ_{max} was again less than 0.001. No anomalies were encountered in the refinement of the structure. The relevant parameters for crystal data, data collection, structure solution, and refinement are summarized in Table 1, and important bond lengths and bond angles are presented in Table 2. A complete description of the details of the crystallographic methods is given in the Supporting Information.

Results and Discussion

Ligand Syntheses. The ligand syntheses are summarized in Schemes 1−4. The ligand **L1** was prepared by Phillips condensation according to the published procedure[19] with minor modification. Subsequently, ligand **L1** was reacted with ethyl bromoacetate in DMF under argon to give the ethyl ester derivative **L2** (Scheme 1). In contrast to **L2**, the methyl ester **L3** was synthesized using direct reductive amination of 1-(methylformyl)benzimidazole with aminoacetic acid methyl ester. The reaction was performed in DCE using sodium triacetoxyborohydride as a robust and effective reducing agent (Scheme 2). In comparison to the method used to prepare **L2**, the synthesis of **L3** only involves one step. Other advantages are shorter reaction time, easier workup and higher yield. Ligand **L4** was prepared by a procedure similar to that of ligand **L3** except that 2-quino-

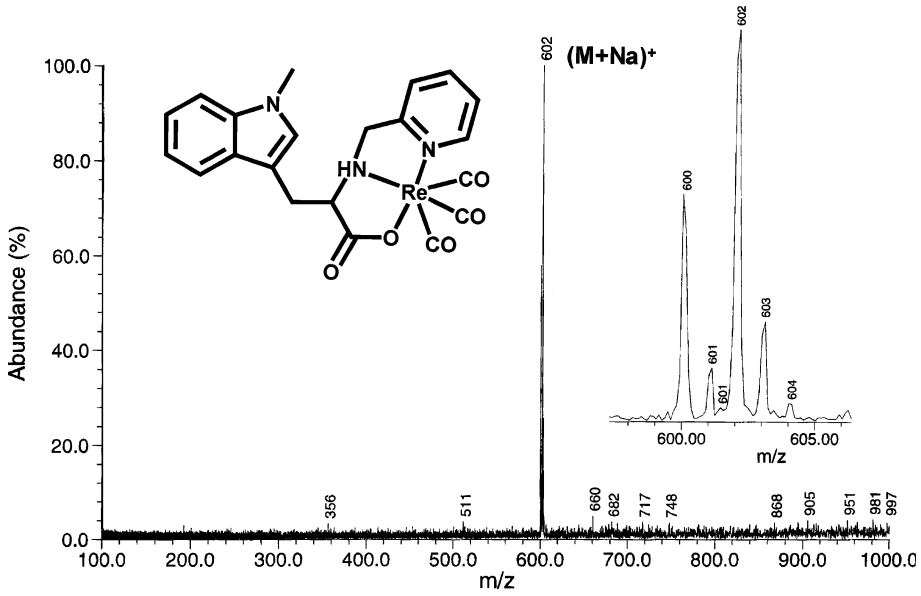

Figure 1. MS spectrum of complex **5**.

Scheme 4

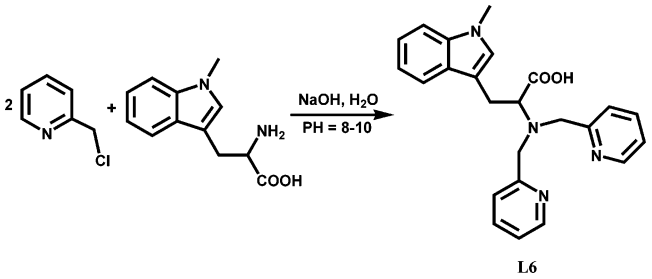

linecarboxaldehyde was used instead of 1-(methylformyl)-benzimidazole.

Following the direct reductive amination procedure, we prepared the bis(quinolinyl) derivative of 1-methyl-L-tryptophan, **L7** (Scheme 3). However, attempts to make the bis-(pyridyl) derivative of 1-methyl-L-tryptophan using the same procedure were not successful. Even though 2 equiv of 2-pyridinecarboxyaldehyde was used, only the mono(pyridyl) derivative **L5** was isolated instead of bis(pyridyl) derivative. The bis(pyridyl) derivative **L6** was synthesized by reacting 2 equiv of 2-(chloromethyl)pyridine with 1-methyl-L-tryptophan under basic conditions (Scheme 4).

Syntheses of the Rhenium Complexes and Their Spectroscopic Properties. The rhenium complexes **1**−**7** were prepared in excellent yields by reacting equivalent amounts of ligands **L1**−**L7** and $[NEt_4]_2[Re(CO)_3Br_3]$ in methanol for 3 h. Single crystals suitable for X-ray crystallography were obtained by slow diffusion of hexane or pentane into solutions of the complexes in dichloromethane or by slow cooling of the methanol solution of the complex.

The IR spectra of the complexes exhibit a sharp, strong band in the 2020−2032-cm^{-1} range and a broad, intense absorption in the 1878−1932-cm^{-1} range, attributed to ν-(C−O) of the *fac*-$\{Re(CO)_3\}^+$ unit.[23] The HRMS spectra of the complexes are consistent with those of the formulations from the elemental analysis and from the spectroscopic evidence. The highest *m*/*z* peaks are assigned to the $[Re(CO)_3(L)]^+$ parent ions on the basis of the isotopic distribution of ^{185,187}Re. The MS spectrum of neutral complex **5** is shown in Figure 1. The most prominent *m*/*z* value corresponds to $(M + Na)^+$ from NaCl added to the solution of the complex in methanol to obtain the MS spectrum.

NMR spectra provide additional evidence for the proposed compositions and molecular structures of the ligands and of the corresponding rhenium complexes. The assignments of all protons are based on the intensity, the spin−spin splitting structure, and $^1H-^1H$ COSY spectroscopy and are presented in the Experimental Section. A significant observation for the structure of the coordination complexes is that the proton signals of the groups close to the rhenium center display downfield shifts for the rhenium complexes compared to the ligands. For ligands **L1**−**L4**, the proton signals of the methylene groups adjacent to the benzimidazole and quinoline groups are singlets in the 4.01−4.16 ppm range. After the ligands have been coordinated to rhenium, these proton signals are split into two sets of doublets in the regions 5.05−5.64 and 4.86−5.28 ppm, with coupling constants consistent with geminal coupling ($J \approx 17$ Hz).

Because of the chiral center on the tryptophan group, NMR spectra of the tryptophan derivatives (ligands **L5**−**L7** and complexes **5**−**7**) display different patterns. For ligands **L5**−**L7**, the proton signals adjacent to the pyridine and quinoline rings are two sets of doublets in the 4.12−4.30 ppm range because these protons are close to the chiral center. After coordination to rhenium, these protons exhibit two sets of multiplets in the region 4.32−5.65 ppm. The hydrogen atoms of the chiral center on the tryptophan groups appear as a quartet for ligand **L5** (3.89 ppm, $J = 9$ Hz) and as triplets for ligands **L6** (3.93 ppm, $J = 7.5$ Hz) and **L7** (4.10 ppm,

(23) (a) Anderson, P. A.; Keene, F. R.; Horn, E.; Tiekink, E. R. T. *Appl. Organomet. Chem.* **1990**, *4*, 523. (b) Abel, E. W.; Ouell, K. G.; Osborne, A. G.; Pain, H. M.; Sik, V.; Hursthouse, M. B.; Malik, K. M. A. *J. Chem. Soc., Dalton Trans.* **1994**, 3441. (c) Gamelin, D. R.; George, M. W.; Glyn, P.; Grevek, F. W.; Schaffner, K.; Turner, J. J. *Inorg. Chem.* **1995**, *33*, 3246. (d) Granifo, J. *Polyhedron* **1999**, *18*, 1061.

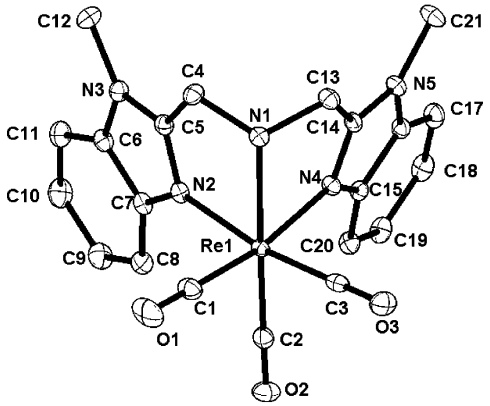

Figure 2. View of the structure of a molecular cation of **1**, showing the atom-labeling scheme and 50% probability ellipsoids.

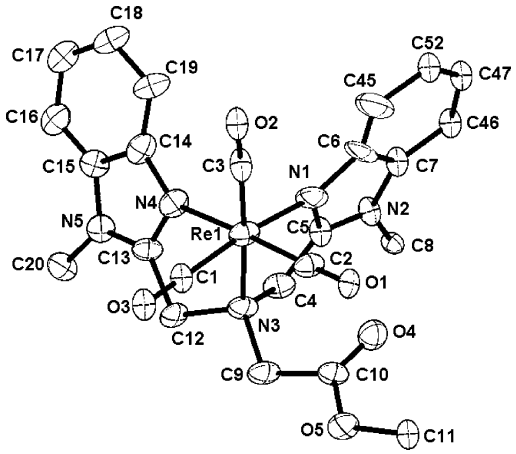

Figure 3. View of the structure of a molecular cation of $\mathbf{3}_2 \cdot NEt_4Br \cdot 8.5H_2O$, showing the atom-labeling scheme and 50% probability ellipsoids.

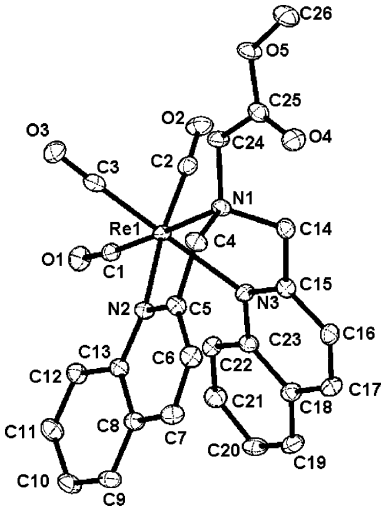

Figure 4. View of the structure of a molecular cation of **4**, showing the atom-labeling scheme and 50% probability ellipsoids.

$J = 8.1$ Hz). In the rhenium complexes **6** and **7**, the proton signals of the chiral center appear as multiplets. The protons signals of the methylene groups adjacent to the indole groups display two sets of multiplets for both the ligands and the rhenium complexes.

^{13}C NMR spectra of complexes **1**−**4** reveal that there are two CO peaks in the 193−198 ppm range. The characteristic 2:1 peak height for these CO resonances indicates that the two CO groups are magnetically equivalent because of the mirror symmetry of the complexes. Also, there is only one set of aromatic proton and carbon signals for complexes **1**−**4**, consistent with the mirror symmetry. Complex **5** shows three CO peaks with equal intensity in the 196−197 ppm range, as is expected for this unsymmetrical neutral complex. For complexes **6** and **7**, although the *fac*-$\{Re(CO)_3\}^+$ coordination cores are symmetric, their ^{13}C NMR spectra show three carbonyl peaks in the 193−196 ppm range because of the chiral center on the tryptophan group. Similar chiral center influence of the NMR spectral pattern has also been observed for the rhenium tricarbonyl complexes of a series of nucleoside derivatives.[24]

Crystallographic Studies. The X-ray structural results confirm that the Re(I) complexes exhibit the chemically robust *fac*-$\{Re(CO)_3\}^+$ core and distorted octahedral geometries. The structure of complex **1** exhibits a discrete bromine anion and the $[Re(CO)_3(\mathbf{L1})]^+$ molecular cation, as shown in Figure 2. The Re(I) site is coordinated to three carbonyl donors in a facial arrangement and to the benzimidazole nitrogen and the amine nitrogen of the ligand to give $\{Re(CO)_3N_3\}$ coordination. The Re−CO bond distances [1.909(2)−1.927(2) Å] are consistent with those found in similar complexes.[11,25,26] The Re−N1 distance of 2.2274(2) Å is longer than those of 2.1498(2) Å for Re−N2 and 2.1508(2) Å for Re−N4, consistent with sp^3- and sp^2-hybridized nitrogen donors, respectively. The trans angles fall in the range of 170.50(7)−172.90(7)°, showing minor deviations from the idealized octahedral limit. The most significant angular distortions are a consequence of the constraints imposed by the tridentate chelate ligand, which forms five-membered rings with the rhenium center, resulting in N2−Re−N1 and N1−Re−N3 angles of 75.27(6)° and 76.80(6)°, respectively.

The structure of the molecular cation of $\mathbf{3}_2 \cdot NEt_4Br \cdot 8.5H_2O$ illustrates that the $\{Re(CO)_3N_3\}$ core geometry is maintained upon introduction of the methyl ester pendant arm (Figure 3). As shown in Table 2, the bond lengths and bond angles associated with **3** are similar to those of **2**. The metrical parameters of the Re(I) site are unexceptional.

As shown in Figure 4, the structure of the cation of complex **4** is similar to that of **3**, with the exception that the quinoline group is present in place of the benzimidazole group of **3**. The distortions from idealized octahedral geometry reflect the multiple-bond character of the carbonyl groups [Re−C, 1.903(3)−1.919(3) Å; C−O, 1.147(3)−1.160(3) Å], the single-bond character of the sp^3-hybridized amine nitrogens (Re−N1, 2.237(2) Å), the sp^2 character of the quinoline nitrogens (Re−N2, 2.217(2) Å; Re−N3,

(24) Wei, L.; Babich, J. W.; Eckelman, W. C.; Zubieta, J. *Inorg. Chem.* **2005**, *44*, 2198.

(25) (a) Wei, L.; Banerjee, S. R.; Levadala, M. K.; Babich, J.; Zubieta, J. *Inorg. Chem. Acta* **2004**, *357*, 1499. (b) Wei, L.; Banerjee, S. R.; Levadala, M. K.; Babich, J.; Zubieta, J. *Inorg. Chem. Commun.* **2003**, *6*, 1099.

(26) Moya, S. A.; Guerrero, J.; Pastene, R.; Schmidt, R.; Sariego, R.; Sartori, R.; Sanz-Aparicio, J.; Fonseca, I.; Martinez-Ripoll, M. *Inorg. Chem.* **1994**, *33*, 2341.

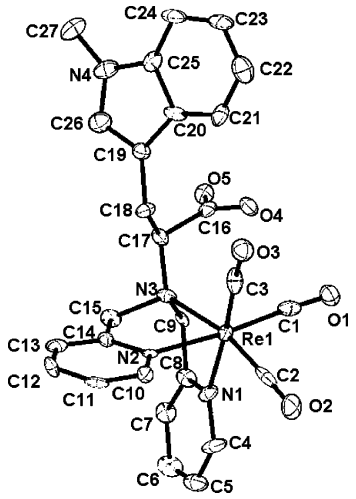

Figure 5. View of the structure of a molecular cation of **6**, showing the atom-labeling scheme and 50% probability ellipsoids.

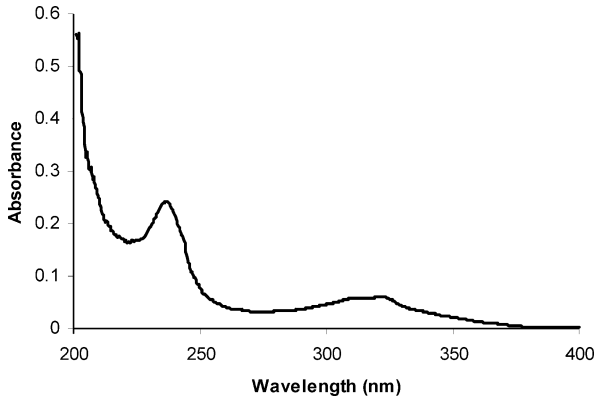

Figure 6. UV spectrum of **4** in ethylene glycol at room temperature.

2.231(2) Å), and the steric constraints imposed by the five-membered chelate rings (Re1−N1−C4−C5−N2 and Re1−N1−C14−C15−N3).

The crystal structure of complex **6** consists of $[Re(CO)_3(\mathbf{L6})]^+$ cations, shown in Figure 5, and discrete Br^- anions. The distorted octahedral environment of the Re(I) site in the molecular cations is defined by the three facially bound CO groups, the tertiary amine, and the pyridine nitrogen donors of the ligand. The bond distances and bond angles are unexceptional. The tryptophan group is directed away from the Re(I) center and, consequently, no direct or indirect interaction of the tryptophan moiety with the rhenium center was observed. Although the carboxylate oxygen atom is an effective donor to rhenium, the structure shows that the $\{Re(CO)_3\}^+$ core exhibits a coordination preference for pyridyl nitrogen rather than the carboxylate unit of the tryptophan group.

UV and Luminescence Spectroscopy. UV and luminescence spectra of complexes **3**, **4**, **6**, and **7** were measured in ethylene glycol at room temperature. As shown in Figure 6 and Table 3, the absorption spectrum of complex **4** displays two peaks. On the basis of previously reported spectroscopic studies of rhenium tricarbonyl complexes,[27−29] we tentatively

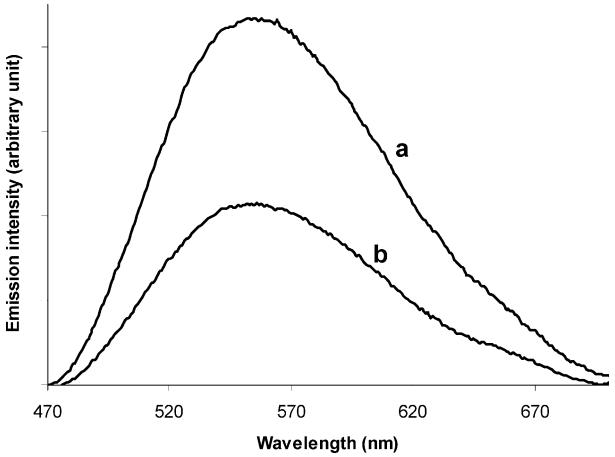

Figure 7. Emission spectra of complex **4** in ethylene glycol at room temperature: (a) N_2-equilibrated; (b) air-equilibrated.

Table 3. Electronic Absorption Data for Complexes **3**, **4**, **6**, and **7** in Ethylene Glycol at Room Temperature

complex	λ_{abs}/nm (ϵ/dm^3 mol^{-1} cm^{-1})
3	214 (28 558), 274 sh (9892), 282 (10 950)
4	235 (23 645), 308 sh (9515), 320 (9955)
6	223 (30 030), 271 (10 100), 289 (9075)
7	234 (20 770), 310 sh (9700), 321 (9795)

assigned the absorption peaks. The intense absorption at 235 nm is related to intraligand (IL) transitions ($\pi-\pi^*$) because a similar absorption is observed for the uncoordinated ligand. The less intense and lower-energy absorption at 320 nm is assigned to a metal-to-ligand charge-transfer (MLCT) d π-(Re)$-\pi^*$(ligand) transition. This transition has some IL character because the free ligand also absorbs in this region.

The steady-state emission spectrum of complex **4** was measured from 350 to 750 nm with an excitation wavelength of 320 nm in 1-nm step size with an integration time of 1 s and a band-pass of 2 nm. As shown in Figure 7 and Table 4, excitation of complex **4** at 320 nm gives rise to an emission peak at 555 nm in ethylene glycol in the presence or absence of air. On the basis of previous spectroscopic studies on the rhenium tricarbonyl complexes,[27−29] the emission peak is assigned to a MLCT transition. The quantum yield of the emission depends on the degree of quenching due to the presence of dissolved oxygen in the sample. Equilibration of the sample in a nitrogen gas atmosphere dramatically increases the quantum yield of the complex from 0.008 to 0.022 (Figure 7 and Table 4). The quantum yields of complex

(27) Lo, K. K. W.; Tsang, K. H. K.; Hui, W. K.; Zhu, N. *Chem. Commun.* **2003**, 2704.

(28) (a) Koike, K.; Tanabe, J.; Toyama, S.; Tsubaki, H.; Sakmoto, K.; Westwell, J. R.; Johnson, F. P. A.; Hori, H.; Saitoh, H.; Ishitani, O. *Inorg. Chem.* **2000**, *39*, 2777. (b) Moya, S. A.; Guerrero, J.; Pastene, R.; Schmidt, R.; Sanz-Aparicio, J.; Fonseca, I.; Martinez-Ripoll, M. *Inorg. Chem.* **1994**, *33*, 2341. (c) Christesen, P.; Hammet, A.; Muir, A. V. G.; Timney, J. A. *J. Chem. Soc., Dalton Trans.* **1992**, 1455. (d) Sun, S. S.; Lees, A. J. *J. Am. Chem. Soc.* **2000**, *122*, 8956. (e) Otsuki, J.; Tsujino, M.; Lizaki, T.; Araki, K.; Seno, M.; Takatera, K.; Watabnabe, T. *J. Am. Chem. Soc.* **1992**, *119*, 7895.

(29) (a) Wong, K. M. C.; Lam, S. C. F.; Ko, C. C.; Zhu, N.; Yam, V. W. W.; Roué, S.; Lapinte, C.; Fathallah, S.; Costuas, K.; Kahlal, S.; Halet, J. F. *Inorg. Chem.* **2003**, *42*, 7086. (b) Yam, V. W. W.; Wong, K. M. C.; Chong, S. H. F.; Lau, V. C. Y.; Lam, S. C. F.; Zhang, L.; Cheng, K. K. J. *Organomet. Chem.* **2003**, *670*, 205. (c) Yam, V. W. W.; Chong, S. H. F.; Ko, C. C.; Cheung, K. K. *Organometallics* **2000**, *19*, 5092.

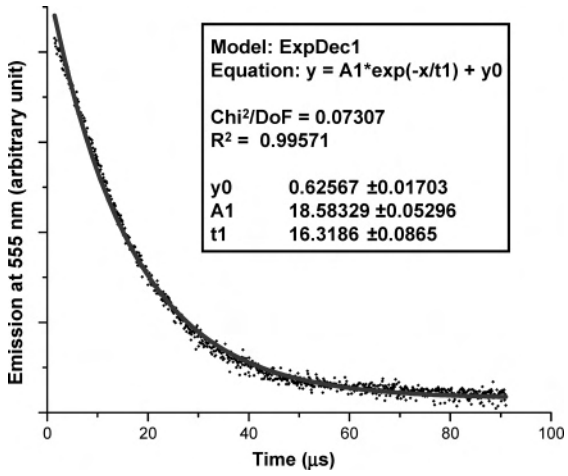

Figure 8. Emission decay trace and monoexponential fit, monitoring at 555 nm in ethylene glycol, for complex **4** at room temperature, after 320-nm excitation. Inset: equation for the monoexponential fit and related parameters, giving a lifetime of $\tau = 16.3$ μs.

Table 4. Photophysical Data for Complexes **3**, **4**, **6**, and **7** in Ethylene Glycol at Room Temperature

complex	medium	λ_{ex}, nm	λ_{em}, nm	Φ	τ, μs
3	N_2-equilibrated	280	575	0.0077	15.40 ± 0.05
	air-equilibrated	280	575	0.0021	
4	N_2-equilibrated	320	555	0.022	16.30 ± 0.10
	air-equilibrated	320	555	0.0080	
6	N_2-equilibrated	290	327	0.048	
	air-equilibrated	290	327	0.045	
7	N_2-equilibrated	320	440	0.021	
	air-equilibrated	320	440	0.023	

4 are comparable to those of the previously reported transition-metal-based fluorescence probes.[27−32]

Lifetime measurement by phosphorescence decay was performed in a degassed solution of complex **4** with excitation and emission wavelengths of 320 and 555 nm, respectively (20-nm band-pass). Figure 8 shows the emission decay spectrum of complex **4**. The complex exhibits single-exponential decay with an emission lifetime of 16.3 μs. The observation of long emission lifetime (on the microsecond time scale), relatively high luminescence quantum yields, and large Stokes' shift suggests that the $Re(CO)_3$−bis(quinoline) complex is a promising candidate for the development of a fluorescence probe for monitoring biological processes in vitro.

Complex **3** shows two absorption peaks at shorter wavelengths compared to those of complex **4** (Table 3). When excited at 280 nm, complex **3** displays an emission peak at 575 nm, which can be logically assigned to a MLCT transition (Table 4). The quantum yield of complex **3** is lower than that of complex **4**, suggesting that complex **3** is a weaker emitter. Therefore, the rhenium−tricarbonyl bis(quinoline) derivative is a better choice for applications as a fluorescence probe. As was observed for complex **4**, oxygen also quenches the MLCT emission of complex **3**. The emission lifetime (15.4 μs) of complex **3** is similar to that of complex **4**, consistent with the long emission lifetimes of MLCT emissions.

As noted in Table 3, we also investigated the UV and fluorescent properties of the tryptophan complexes **6** and **7**. The UV spectrum of complex **6** exhibits three absorption peaks. The complex shows a typical tryptophan emission at 327 nm (Table 4) with a quantum yield of 0.048 at $\lambda_{ex} =$ 290 nm. This emission may be related to intramolecular energy transfer or to the direct excitation of the pendant tryptophan group. Because this emission does not arise from a MLCT transition, oxygen quenching is not observed. Similar quantum yields for the N_2- and air-equilibrated samples were observed.

Complex **7** shows absorption peaks similar to those of complex **4** (Table 3), but curiously the emission spectra of **4** and **7** are different. Upon excitation at 320 nm, complex **7** exhibits an emission at 440 nm with a quantum yield of 0.02 and no oxygen-quenching effect (Table 4). The absence of an emission for **7** at 555 nm, as found for **4**, suggests that the tryptophan group quenches the MLCT emission of the $Re(CO)_3$−bis(quinoline) chromophore. Similar emission quenching was also observed for the $Re(CO)_3$−phenanthroline complexes by the indole group.[27] On the other hand, complex **7** does not exhibit a typical tryptophan emission at ca. 330 nm, rather showing an emission at 440 nm. It is likely that the tryptophan emission is absorbed by the complex itself given the rather intense absorption of the complex at 321 nm. Similarly, the unusual emission band at 440 nm might be related to some type of interaction between the tryptophan and quinoline groups. This interaction may be minimized by adding a spacer between the two groups.

Because the emissions of complexes **6** and **7** are not related to MLCT, the lifetimes are much shorter than those of complexes **3** and **4**. In fact, because of the limitation of the spectrofluorometer, we could not measure the lifetimes of complexes **6** and **7**.

Trace amounts of ligand impurities in the complexes may also contribute to the unusual photophysical properties of complexes **6** and **7**. While our experimental results do not completely exclude the possibility of small amounts of impurities in the samples, NMR and elemental analyses are consistent with sample purity.

Conclusions

A series of tridentate ligands derived from quinoline, benzimidazole, and tryptophan have been developed. The ligands react cleanly and in high yields with $[NEt_4]_2[Re(CO)_3Br_3]$ to give cationic complexes $[Re(CO)_3(\mathbf{L}x)]Br$ ($x = \mathbf{1}-\mathbf{4}$, **6**, and **7**) and the neutral complex $[Re(CO)_3(\mathbf{L5})]$. The structures of the complexes display distorted octahedral

(30) (a) Hu, X.; Smith, G. D.; Sykora, M.; Lee, S. J.; Grinstaff, M. W. *Inorg. Chem.* **2000**, *39*, 2500. (b) Beilstein, A. E.; Tierney, M. T.; Grinstaff, M. W. *Comments Inorg. Chem.* **2000**, *22*, 105. (c) Kahn, S. I.; Beilstein, A. E.; Grinstaff, M. W. *Inorg. Chem.* **1999**, *38*, 418. (d) Krider, E. S.; Rack, J. J.; Frank, N. L.; Meade, T. J. *Inorg. Chem.* **2001**, *40*, 4002.

(31) Rack, J. J.; Kirder, E. S.; Meade, T. J. *J. Am. Chem. Soc.* **2000**, *122*, 6287. (b) Krider, E. S.; Miller, J. E.; Meade, T. J. *Bioconjugate Chem.* **2002**, *13*, 155.

(32) (a) Bannwarth, W.; Schmidt, D. *Tetrahedron Lett.* **1989**, *30*, 1513. (b) Magda, D.; Crofts, S.; Lin, A.; Miles, D.; Wright, M.; Sessler, J. L. *J. Am. Chem. Soc.* **1997**, *119*, 2293. (c) Meggers, E.; Kusch, D.; Giese, B. *Helv. Chim. Acta* **1997**, *80*, 640. (d) Khan, S. I.; Beilstein, A. E.; Smith, G. D.; Sykoram, M.; Grinstaff, M. W. *Inorg. Chem.* **1999**, *38*, 3922.

geometries, with the three carbonyl donors in the facial orientation. The bis(quinoline) derivative **4** displays luminescence at 555 nm, assigned to MLCT, with a long emission lifetime, relatively high quantum yield, and a large Stokes' shift, suggesting that the complex is an ideal fluorescence probe for in vitro imaging studies. The bis(benzimidazole) derivative **3** is a weaker emitter than complex **4**. Complex **6** exhibits a typical tryptophan emission, while the luminescence spectrum of complex **7** exhibits an interaction between the quinoline and tryptophan moieties. The luminescence properties of the $Re(CO)_3$−bis(quinoline)−tryptophan derivatives may conceivably be improved by introducing a spacer between the bis(quinoline) and tryptophan units, an aspect of the work that is under investigation. Because the unusual photophysical properties of complexes **6** and **7** may arise from a variety of factors, further investigations of the spectroscopy of these and related compounds are in progress.

Acknowledgment. This work was supported by a grant from the National Institutes of Health, National Institute of Allergy and Infectious Diseases (Grant STTR 1R41 A1044080-01).

Supporting Information Available: X-ray crystallographic files in CIF format and MS spectra of complexes **1**, **4**, and **6**. This material is available free of charge via the Internet at http://pubs.acs.org.

IC0517319